Thermochimica Acta, 183 (1991) 313–321
Elsevier Science Publishers B.V., Amsterdam

Differential scanning calorimetry of the triphosphoinositide–water system [α]

Toshiharu Takizawa [a], Kohei Hayashi [b] and Hiroshi Mitomo [c]

[a] *Department of Physics, Faculty of General Studies, Gunma University, Maebashi (Japan)*
[b] *Department of Physiology, Faculty of Education, Ibaraki University, Mito (Japan)*
[c] *Department of Biological Engineering, Faculty of Engineering, Gunma University, Kiryu (Japan)*

(Received 14 September 1990)

Abstract

Triphosphoinositide (TPI) (Phosphatidylinositol-4,5-bis-(phosphate) (PIP_2)) is an acidic phospholipid occurring at high levels in nerve tissues, which has attracted special interest concerning nerve excitation and cell signalling. In our differential scanning calorimetric study of the PIP_2–water system and a broad endothermal peak was observed. The transitional enthalpy increases rapidly with an increase in the ratio of water to PIP_2. The endothermal transition displays a strong hysteresis in the heating and cooling cycles in differential scanning calorimetry. An NMR study of an aqueous dispersion of PIP_2 revealed that the endothermal transition cannot be attributed to a gel to liquid–crystal transformation. We postulated a thermal dehydration mechanism for the PIP_2–water system, based on the model of the internally hydrated PIP_2 bilayer reported in a previous paper.

INTRODUCTION

Triphosphoinositide (TPI) (phosphatidylinositol-4,5-bis(phosphate) (PIP_2) is a phospholipid with a high solubility in water; it is present at high levels in the cell membranes of brains and kidneys [1]. Biochemists first studied PIP_2 in connection with nerve excitation [2,3]; today they concentrate their attention on PIP_2 as the source of the secondary messenger in cell signalling [4].

Previously, we studied the mixing enthalpies of aqueous dispersions of PIP_2 with $CaCl_2$ solutions and assumed that the water molecules penetrate into the hydrophobic spaces between the hydrocarbon chains of the PIP_2 bilayers when the ionic part of PIP_2 is free from Ca^{2+} ions [5,6]. In this paper we report the results of the DSC of PIP_2–water systems which

[α] Paper presented at the Second Japan–China Joint Symposium on Calorimetry and Thermal Analysis, 30 May–1 June 1990, Osaka, Japan.

0040-6031/91/$03.50

revealed a new type of phase transition in phospholipid–water systems. The results strongly support the existence of hydrophobic hydration in the phospholipid–water system.

MATERIALS AND METHODS

PIP_2 was obtained by Folch fractionation of bovine brain [7]. The crude extract was purified further by chromatography on DEAE-cellulose according to the method of Hendrickson and Ballow [8], and the ammonium salt of PIP_2 was obtained. The PIP_2 bound with divalent cations was removed in the above preparation process. The prepared sample gave a single spot on a thin layer chromatography plate. A PIP_2 sample whose monovalent cations were partially replaced by Ca^{2+} ions was prepared by adding $CaCl_2$ solution to an aqueous dispersion of PIP_2, producing a liophilized PIP_2 powder bound with an equimolar amount of calcium. Dipalmitoyl-phosphatidylcholine (DPPC) was obtained from Sigma Chemical Co.

The water contents of the samples for DSC measurement were adjusted by exposing freeze-dried samples of PIP_2 to an atmosphere of saturated water vapour at 4 °C for a pre-set time; the water contents were determined gravimetrically. For higher water contents, however, distilled water was added directly to the freeze-dried powder in a sample cell and the mixture was stirred with a fine needle.

DSC measurements were carried out using a Seiko SSC-540 heat-conduction scanning microcalorimeter, which utilizes Melcor thermomodules consisting of semiconductor thermopiles as a sensitive detector for the heat flow. The performance of the furnace was improved with the aid of Tokyo Riko Ltd. A silver cell with a net volume of 70 μl was sealed to prevent evaporation of moisture by pressing down and squeezing a tapered silver cover. The weight of dry sample used in a DSC measurement was 2–5 mg, and the heating rate was 200 s $^{\circ}C^{-1}$, at which the baseline was flat, even near the starting temperature.

Special caution was taken not to heat the sample over 60 °C, because chemical change occurs at higher temperatures [9]. Ultrasonication was carried out in ice water for PIP_2, and at 50 °C for DPPC. A JNM-FX 90Q FT-NMR was used to obtain NMR spectra of an aqueous dispersion of PIP_2 for comparison with those of DPPC.

RESULTS

DSC curves of aqueous dispersions of PIP_2 with various thermal hysteresses and treatments are shown in Fig. 1. The curve A represents the thermogram obtained for the first run starting from above the freezing

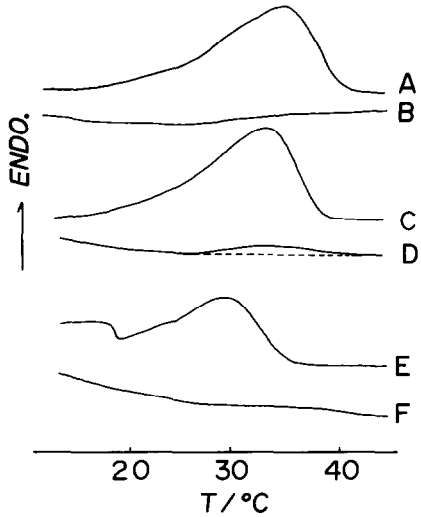

Fig. 1. Various DSC thermograms of aqueous dispersions of PIP_2 (7.6 wt.% PIP_2; sample, batch No. 1): A, initial scan; B, second scan, started from above the freezing point immediately after the initial scan; C, third scan started from below the freezing point; D, scan for the same sample kept for 1 day at 0 °C and started from above the freezing point; E, the same sample started at −40 °C, sonicated at 0 °C and started from above the freezing point; F, initial scan for PIP_2 bound with an equimolar amount of calcium.

temperature of the dispersion to 45 °C. The second run was carried out immediately after the sample had cooled down to the initial starting temperature, and thermogram B was obtained. A broad endothermal peak is observed in the former thermogram in the temperature range 10–40 °C, but not in the latter. When the same sample was cooled down below the freezing point of the dispersion, however, a broad endothermal peak appeared again, as shown in thermogram C. A partial recovery, as shown in curve D, was observed when the heated sample was kept at a low temperature above the freezing point for a long time (about several days).

The viscosity of the aqueous dispersion of PIP_2 drops drastically following both ultrasonication and heating. Ultrasonication, however, did not change the main feature of the DSC curve of the aqueous dispersion of PIP_2 (thermogram E), although the baseline at a lower temperature is much higher than that in curve A. A DSC thermogram of an aqueous dispersion of calcium-bound PIP_2 has no endothermal peak as shown in curve F.

Figure 2 shows the DSC curve of a wet PIP_2 powder, in which the endothermal hysteresis seen in Fig. 1, with respect to the appearance of the endothermal peaks, is also observed.

Figure 3 shows thermograms for PIP_2–water systems with various water contents, obtained as the initial DSC runs. No endothermal peak was found in a dry sample up to 60 °C (even up to 100 °C). Previously, we had observed an exothermic peak at about 60 °C for liophilized dry PIP_2 powder

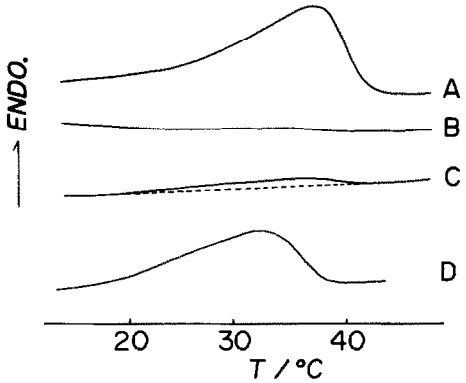

Fig. 2. Thermal hysteresis of DSC thermograms of a PIP_2–water system (weight ratio of H_2O to PIP_2, 1.7; sample, batch No. 1): A, initial scan; B, second scan starting from above the freezing point; C, kept at 0 °C for 2 days; D, final DSC scan starting from above the freezing point.

in contact with air, and the peak was attributed to the oxidation of PIP_2. Therefore the DSC scan was usually stopped before reaching 60 °C. The characteristic patterns of the endothermal peaks for PIP_2–water systems do not change with a decrease in the weight ratio of water in the sample, but the endothermal peaks shift gradually to higher temperatures as the weight ratio of water decreases.

All the results reported above were obtained from PIP_2 samples from the same batch obtained in one extraction process. Although the main characteristic of the endothermal phase transition of the PIP_2–water system is the same for various batches obtained from different sources of brains, the profiles and positions of the endothermal peaks and their thermal hystereses are somewhat different among samples from different batches. Thermo-

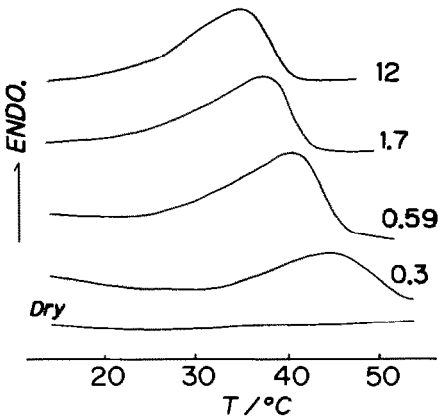

Fig. 3. Effect of water content on DSC thermograms of PIP_2–water systems. Weight ratios of H_2O to PIP_2 are indicated on the figure; sample, batch No. 1.

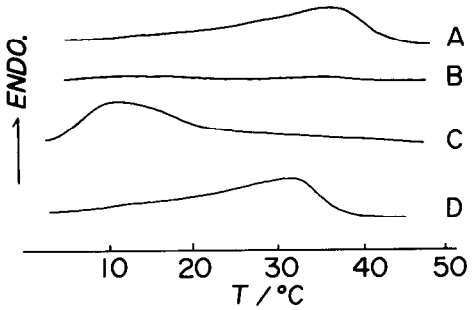

Fig. 4. Thermal hysteresis of DSC thermograms of an aqueous dispersion of PIP_2 for another batch of PIP_2 (sample, batch No. 2; 6.2 wt.% PIP_2): A, initial scan; B, scan started from above the freezing point; C, scan after storing at 0 °C (above the freezing point of the dispersion) for one day; D, final scan started from below the freezing point.

grams with characteristics differing from the preceding results both in the endothermal peak profile and in the hysteresis are shown in Figs. 4 and 5. When the DSC samples of PIP_2–water systems are stored at 0 °C after the first run to 45 °C, thermal recover to the initial state is more rapid than the result shown in Figs. 1 and 2.

The temperature dependences of the NMR signals of aqueous dispersions of PIP_2 and DPPC are shown in Figs. 6 and 7. Proton signals of CH_2 and CH_3 in acyl groups of PIP_2 are observed even below the endothermal transition temperature, and no significant change occurs following the endothermal transition. In contrast to the case of PIP_2, proton signals from CH_2 and CH_3 in acyl groups of DPPC are scarcely discerned at room

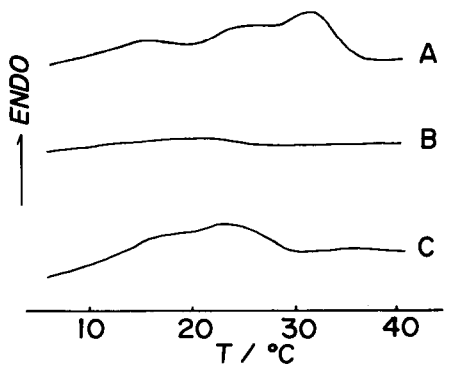

Fig. 5. Thermal hysteresis of DSC thermograms of PIP_2–water systems (sample, batch No. 3; weight ratio of H_2O to PIP_2, 0.42): A, initial scan; B, immediately after the initial scan; C, after storage at 0 °C for 1 day.

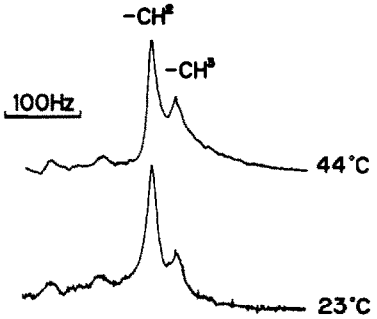

Fig. 6. Temperature dependence of NMR signals of an aqueous dispersion of PIP_2–NH_4; sample, batch No. 1. Signal positions of CH_2 and CH_3, and the temperatures of the sample are indicated on the figure.

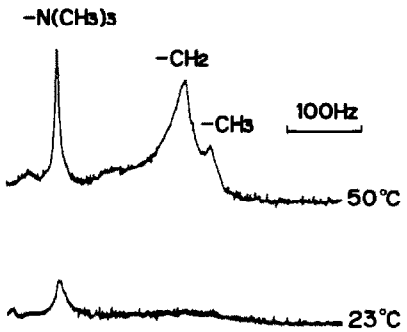

Fig. 7. Temperature dependence of NMR signals of an aqueous dispersion of DPPC.

temperature, and appear clearly after the main transition of DPPC is complete at about 42° C.

DISCUSSION

Broadly speaking, there are two types of phase transition in phospholipid–water systems. One is a gel to liquid-crystal transition which arises from a change in the molecular motions of the lipid molecules in a definite molecular aggregated structure. The other is a transition from one aggregated form of lipid molecules to another, such as a hexagonal rod to lamella transition.

High resolution proton magnetic resonance signals of acyl groups of PIP_2 can be observed even below the phase transition temperature of PIP_2–water systems, implying that rapid motion of acyl chains occurs even below the phase transition temperature. Moreover, there is no significant increase in the signal intensity following the endothermal transition, in contrast to the DPPC–water system in which the molecular motions of the acyl chains are released after the main transition at 42° C. These facts clearly suggest that the endothermal transition of the PIP_2–water system is not a gel to liquid-

crystal phase transition.

The transition does not, however, reflect a structural change between hexagonal rod and lamella, because the X-ray diffraction study of PIP_2–water systems revealed that the lamella structure is maintained before and after the endothermal transition in the DSC scan [10].

The endothermal transition of PIP_2–water systems has a remarkable hysteresis, as shown in the DSC thermograms. A well-known thermal hysteresis in the DSC of the phospholipid–water system is observed at the subtransition of DPPC in which recovery from a gel state ($L_{\beta'}$) to a crystalline state (L_c) is very slow [11].

However, the endothermal transition in PIP_2–water systems cannot be this type of transition because the acyl chains move rapidly, even below the transition temperature, and the rate of rearrangement of acyl chains may be too rapid to form a crystalline state. Ultrasonication does not alter the basic characteristic of the endothermal transition of PIP_2–water systems as shown in Fig. 1. The result implies that the transition does not belong to a mere reorganization of the aggregated structures of the PIP_2 molecules.

Previously, we have studied the heat of mixing of aqueous dispersions of PIP_2 with $CaCl_2$ solutions at 20 °C, and deduced that the acyl chains of PIP_2 molecules contribute positively to the mixing enthalpies and entropies. The contribution of the acyl chains to the mixing enthalpies reached 30 kJ mol^{-1} of PIP_2. Assuming water penetration into the hydrophobic spaces among the acyl chains of the PIP_2 bilayers, the positive contributions of the acyl chains were attributed to the exclusion of water from the hydrophobic interior of the PIP_2 membranes as a result of the decrease in occupied area per PIP_2 molecule caused by the neutralization effect of the Ca^{2+} ions on the negative surface charge of the PIP_2 bilayers. The endothermal DSC transition of the PIP_2–water system can be attributed to the same dehydration mechanism, although it is induced by heating in this case. The schematic representation of the phase transition of the PIP_2–water system is as follows:

$$\text{Loosely packed bilayer} \underset{-Ca^{2+},\ \text{cooling (hydration process)}}{\overset{+Ca^{2+},\ \text{heating (dehydration process)}}{\rightleftharpoons}} \text{Tightly packed bilayer}$$

In general, hydrophobic interactions among molecules increase with an increase in temperature [12]. Endothermal phase transitions of PIP_2–water systems in DSC may be brought about by an increase in the hydrophobic strength between the PIP_2 molecules in water as the temperature increases.

The enthalpies of the phase transitions of PIP_2–water systems were estimated from the endothermal peak area of the DSC curves in Fig. 3 and are plotted in Fig. 8 as a function of the water content. The transitional enthalpy increases rapidly at first with an increase in water content from zero to 7.1 kcal mol^{-1} at a water content of 0.6, then increases gradually up to 8.4 kcal mol^{-1} at a water content of 1.7.

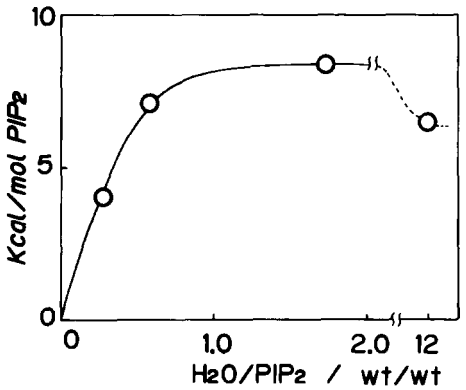

Fig. 8. Effect of water content on the thermal transition enthalpies of PIP_2–water systems; sample, batch No. 1.

The thermal transition enthalpy of the aqueous dispersion of PIP_2 is 6.5 kcal (27 kJ) mol^{-1} of PIP_2 as shown in the figure. This magnitude is close to the enthalpy of Ca^{2+} binding to the aqueous dispersion of PIP_2, as mentioned above. This implies that the complete exclusion of water from the hydrophobic interior of the bilayer of PIP_2 is achieved by both an addition of Ca^{2+} ions and an elevation of temperature.

A DSC curve of an aqueous dispersion of PIP_2 whose monovalent ammonium ions are partially replaced by Ca^{2+} ions has no endothermal peak, as shown in the result in Fig. 1. The Ca^{2+} ions have a strong neutralization effect on the surface of the PIP_2 bilayer, and exclusion of water from the interior of the lamella is complete even at the low end of the temperature range (20 °C) when equimolar Ca^{2+} ions bind to the ionic groups of PIP_2.

As shown in Fig. 1, the heat capacity of sonicated PIP_2 dispersions is much higher at a low temperature than that of the unsonicated sample. It is known that sonication produces disorder within a lipid bilayer, because some constraints are produced by the small radius of curvature of the vesicles [13]. Some of the penetrated water may be released at a lower temperature before the phase transition, because of the looser surface structure of the sonicated vesicles.

Recently, we have carried out a neutron diffraction study of the PIP_2–water system; the results support the presence of penetrated water in the hydrophobic region of the PIP_2 bilayer at low temperatures and the exclusion of water from the inside of the bilayer as a result of heating [14].

Finally, there is a most striking difference in the characteristics of the endothermal transitions shown in Figs. 4 and 5, compared with those in Figs. 1 and 2, in the recovery process at 0 °C; the recoveries in Figs. 4 and 5 are prominent, and the endothermal transitions occur at a low temperature in successive DSC scans after the recovery at 0 °C. Such large shifts in peak

temperatures may be explained with a modification of our model of the phase transition of PIP_2–water systems.

Here we assume two kinds of surface structure for PIP_2 bilayers in water: the surface structures at low temperature (SL) and at high temperature (SH). The surface structure of the bilayer changes from SL type to SH type during the transition in the first DSC scan. When the temperature is reduced below the freezing point of the PIP_2–water systems, the surface structure of the PIP_2 bilayers returns to SL type. However, when the sample is merely cooled down to above the freezing point and held these for a long time, the surface structure remains in the SH form. Water may penetrate gradually through the SH surface at the low temperature above the freezing point, because the hydrophobicity decreases with a decrease in temperature. However, SH-type surfaces are unstable at low temperatures below the phase transition, and the endothermal peaks in the second run appear at a temperature slightly below that in the first run.

The difference in the characteristics of the endothermal transition among the preparation batches of the samples may originate in some unknown differences in the prepared PIP_2 samples, such as fine differences in the residual proton forms in the ionic groups of PIP_2, or some differences in the acyl groups of PIP_2, although we have no structural evidence concerning these differences at the present time.

REFERENCES

1 K. Hayashi, Membrane (Maku, in Japanese), 2 (1977) 86.
2 M. Kai and J.N. Hawthrone, Ann. NY Acad. Sci., 165 (1969) 761.
3 A.C. Birnberger, K.L. Birnberger, S.L. Eliasson and P.C. Simpson, J. Neurochem., 18 (1971) 1291.
4 M.J. Birridge and P.F. Irrine, Nature, 312 (1984) 315.
5 T. Takizawa and K. Hayashi, Gunma Journal of Liberal Arts and Sciences, 17 (1983) 17.
6 T. Takizawa, K. Hayashi, S. Yabuki and Y. Nakata, Thermochim. Acta, 123 (1988) 247.
7 J. Folch, J. Biol. Chem., 177 (1949) 497.
8 H. Hendrickson and C.E. Ballow, J. Biol. Chem., 239 (1964) 1369.
9 T. Takizawa and K. Hayashi, Rep. Prog. Polym. Phys. Jpn., 25 (1982) 773.
10 T. Takizawa, unpublished data, 1989.
11 S.C. Chen, J.M. Sturtevant and B.J. Gaffney, Proc. Natl. Acad. Sci. U.S.A., 77 (1980) 5060.
12 A. Ben-Naim, Hydrophobic Interactions, Plenum, New York, 1980, p. 185.
13 M.P. Sheetz and S.I. Chan, Biochemistry, 11 (1972) 4573.
14 S. Yabuki, T. Takizawa, K. Hayashi, H. Mitomo, N. Niimura and M. Hurusaka, in N. Niimura and M. Hurusaka (Eds.), Proceedings of the Workshop on Structure Study of Biology by X-ray and Neutron Scattering, KEK, Technical Information Library, National Laboratory for High Energy Physics, Tsukuba, Japan, 1989 (in Japanese).